Geomechanics and Engineering, *Vol. 19, No. 4 (2019) 343-352*
DOI: https://doi.org/10.12989/gae.2019.19.4.343

Estimating UCS of cement-grouted sand using characteristics of sand and UCS of pure grout

Changho Lee[1a], Hongyeop Nam[2b], Woojin Lee[2c], Hyunwook Choo*[3] and Taeseo Ku[4d]

[1]*Department of Marine and Civil Engineering, Chonnam National University, Yeosu 550-749, Republic of Korea*
[2]*School of Civil, Environmental and Architectural Engineering, Korea University, Seoul 136-713, Republic of Korea*
[3]*Department of Civil Engineering, Kyung Hee University, Yongin 17104, Republic of Korea*
[4]*Department of Civil and Environmental Engineering, National University of Singapore, 117576 Singapore*

(Received July 12, 2019, Revised November 1, 2019, Accepted November 8, 2019)

Abstract. For quality control and the economical design of grouted sand, the prior establishment of the unconfined compressive strength (UCS) estimating formula is very important. This study aims to develop an empirical UCS estimating formula for grouted sand based on the physical properties of sands and the UCS of cured pure grout. Four sands with varying particle sizes were grouted with both microfine cement and Ordinary Portland cement. Grouted specimens were prepared at three different relative densities and at three different water-to-cement ratios, and unconfined compression tests were performed. The results demonstrate that UCS of grouted sand can be expressed as the power function of the UCS of cured pure grout: $UCS_{grouted\ sand}$ / 1 MPa = A_{soil} · $(UCS_{pure} / 1\ MPa)^N$. Because the exponent N strongly depends on the combination of pore area and pore size, N is expressed as the function of porosity (n) and specific surface (S_a). Additionally, because S_a determines the area of the sand particle that cement particles can adsorb and n determines the number of cementation bondings between sand particles, A_{soil} is also expressed as the function of n and S_a. Finally, the direct relationship between A_{soil} and N is also investigated.

Keywords: grouting; microfine cement; unconfined compressive strength; specific surface; porosity

1. Introduction

Grouting is a method of injecting various cementitious materials into voids, fissures, and cavities in grounds to improve their engineering properties, such as increasing the strength and stiffness and decreasing hydraulic conductivity (Celik 2019, Chang *et al.* 2016, Gopinathan and Anand 2018, Nonveiller 2013). Therefore, grouting has been widely used to achieve various purposes, including increasing the bearing capacity of foundations, enhancing the stability of slopes and underground structures, and mitigating liquefaction susceptibility (Abramson *et al.* 2002, Brachman *et al.* 2004, Dano *et al.* 2004, Gallagher and Mitchell 2002, Gallagher *et al.* 2007, Hoek 2001, Hsiao *et al.* 2016, Li *et al.* 2017, Pantazopoulos and Atmatzidis 2012, Van der Stoel 2001, Zebovitz *et al.* 1989).

Because the grouting method has many uncertainties regarding the control of the shape and position of the grout suspension in the field, the measurement of the unconfined compressive strength (UCS) of the grouted specimen retrieved by coring or sampling from a grouted ground is widely used to identify and judge the quality of the reinforcement or improvement after the injection of grout. However, coring or sampling is an expensive and time-consuming process to prepare the specimen for an unconfined compression test, and it can even disturb the grouted ground. Therefore, for the quality control of the grouted sand, previous researchers have suggested many empirical correlations to estimate the UCS of grouted sand (Avci and Mollamahmutoğlu 2016, Dano *et al.* 2004, Kaga and Yonekura 1991, Markou and Droudakis 2013, Sunitsakul *et al.* 2012, Tinoco *et al.* 2011). Additionally, the establishment of empirical UCS estimating formulas is quite appealing because a prior estimation of the strength of grouted sand before injecting the grout into the sand deposit benefits the economical design of soil stabilization.

The present experimental investigation focuses on suggesting the empirical formula to estimate the UCS of sand grouted with microfine cement using the physical properties of sand such as specific surface and porosity and the UCS of cured pure grout (or cured cement suspension). Therefore, various factors that affect the UCS of cured pure grout such as water-to-cement ratio and cement type, and those determining physical properties of sand such as median particle size and relative density (or porosity) were selected as the testing variables in this study, and a bleeding test, viscosity measurement, and unconfined compression test were performed.

*Corresponding author, Assitant Professor
E-mail: choohw@khu.ac.kr
[a]Associate Professor
E-mail: changho@jnu.ac.kr
[b]Graduate Research Assistant
E-mail: kiok462@naver.com
[c]Professor
E-mail: woojin@korea.ac.kr
[d]Assistant Professor
E-mail: ceekt@nus.edu.sg

http://www.techno-press.org/?journal=gae&subpage=7
ISSN: 2005-307X (Print), 2092-6219 (Online)

2. Background

The unconfined compressive strength of grouted sand ($UCS_{grouted\ sand}$) is controlled by various factors, including the water-to-cement ratio (W/C), relative density (or porosity), particle size, mineralogy, fines content, specific surface of both sand and cement, types of grout, and curing period (Avci and Mollamahmutoğlu 2016, Consoli *et al.* 2007, Kaga and Yonekura 1991, Markou and Droudakis 2013, Ozgurel and Vipulanandan 2005, Zebovitz *et al.* 1989). Table 1 summarizes several existing UCS estimating formulas for grouted sand.

Case 1 in Table 1 is the UCS estimating formula suggested by Kaga and Yonekura (1991) based on the experimental results of sands grouted with a silicate. Kaga and Yonekura (1991) noted that B in Case 1 in Table 1 is the UCS of ungrouted pure sand, and A_{soil} and N are the fitting parameters related to the properties of sand, such as a volumetric specific surface and porosity (n) (or relative density). Therefore, the formula of Kaga and Yonekura (1991) highlights the importance of the UCS of cured pure grout (UCS_{pure}) and the properties of sand to the proper determination of $UCS_{grouted\ sand}$.

Case 2 in Table 1 is the UCS estimating formula suggested by Dano *et al.* (2004) based on the experimental results of Fontainebleau sand grouted with microfine cement at a relative density of around 78%. Note that W/C determines the UCS_{pure}, which will be shown in the later part of this study; therefore, the formula of Dano *et al.* (2004) highlights the importance of the UCS_{pure} to the determination of $UCS_{grouted\ sand}$.

Case 3 in Table 1 is the UCS estimating formula suggested by Ozgurel and Vipulanandan (2005) based on the experimental results of sand grouted with acrylamide. Because the particle size of sand corresponding to 10% pass (D_{10}) is strongly related with the specific surface (S_a) of soils, the formula of Ozgurel and Vipulanandan (2005) implies the importance of S_a and UCS_{pure} to the proper determination of $UCS_{grouted\ sand}$.

Sunitsakul *et al.* (2012) (Case 4 in Table 1) predicted the UCS of sand grouted with cement at 7 days of curing time. Because the California bearing ratio (CBR) is strongly dependent on the packing density of soils, the formula suggested by Sunitsakul *et al.* (2012) highlights the importance of n of sand and the UCS_{pure}, which is determined by W/C, to the determination of $UCS_{grouted\ sand}$.

Markou and Droudakis (2013) (Case 5 in Table 1) proposed the empirical UCS estimating formula of the sand grouted with microfine cement as the function of hydraulic conductivity (k). Because the variation of k can be effectively captured by D_{10} (Hazen equation) or S_a and n (Kozeny-Carman equation) (Choo *et al.* 2018), the formula of Markou and Droudakis (2013) highlights the importance of S_a and n to the determination of $UCS_{grouted\ sand}$.

The comparison of various empirical UCS estimating formulas in Table 1 demonstrates that $UCS_{grouted\ sand}$ is mainly determined by the characteristics of sand and pure grout (S_a, n, and $UCS_{pure\ grout}$). Therefore, the main object of this study is to suggest the UCS estimating formula of grouted sand as the function of S_a, n, and UCS_{pure}.

Table 1 Selected previous UCS estimating formulas for grouted sands

Case	Equations	Reference
1	$\mathbf{UCS_{grouted\ sand} = B + A_{soil} \times (UCS_{pure\ grout})^{N}}$	Kaga and Yonekura (1991)
2	$\mathbf{UCS_{grouted\ sand} = 40 \times \left(\frac{W}{C}\right)^{-2.0}}$	Dano *et al.* (2004)
3	$\mathbf{UCS_{grouted\ sand} = 6.0 \times \left(\frac{D_{10}}{1\ mm}\right)^{-0.35} \times UCS_{pure\ grout}}$	Ozgurel and Vipulanandan (2005)
4	$\mathbf{UCS_{grouted\ sand} = 0.427 \times \left(\frac{CBR}{W/C}\right)^{0.578}}$	Sunitsakul *et al.* (2012)
5	$\mathbf{UCS_{grouted\ sand} = 1.08 \times (k)^{-0.47}}$	Markou and Droudakis (2013)

where $UCS_{grouted\ sand}$ = unconfined compressive strength of grouted sand; $UCS_{pure\ grout}$ = unconfined compressive strength of cured pure grout; W/C = water-to-cement ratio; CBR = California bearing ratio; D_{10} = effective particle size; and k = hydraulic conductivity

3. Experimental program

3.1 Materials

Four angular silica sands (Kyung-In Co., South Korea) were used in this study. The four sands, K3, K4, K5, and K6 have different median particle sizes (D_{50}) ranging from 1.65 mm to 0.47 mm as shown in Fig. 1. No fine particle (<75 μm) is included in the specimen to prevent any potential issue (e.g., clogging) due to fines migration (Zheng *et al.* 2018). All tested sands can be classified as SP (poorly graded sand) according to the unified soil classification system (USCS). Table 2 summarizes index properties of the tested sands. Note that the values of specific surface (S_a = surface area / mass), which were calculated using Eqs. (1) (Santamarina *et al.* 2001) for the tested sands, are also included in Table 2.

$$S_a = \frac{3(C_u + 7)}{4 \cdot \rho_w \cdot G_s \cdot D_{50}} \quad (1)$$

where C_u = uniformity coefficient; ρ_w = mass density of water; and G_s = specific gravity.

Commercially available microfine cement (Ssangyong Company, South Korea) and Ordinary Portland cement (OPC) (Hanil Company, South Korea) were selected to prepare the cement grout suspension. The maximum particle size and specific surface of the microfine cement are finer than 15 μm and greater than 860 m^2/kg, respectively (data from the manufacturer). In the case of OPC, the maximum particle size is around 30 μm, and the specific surface is 280 m^2/kg (data from the manufacturer).

3.2 Sample preparation

Fig. 2 shows the sample preparation equipment used in

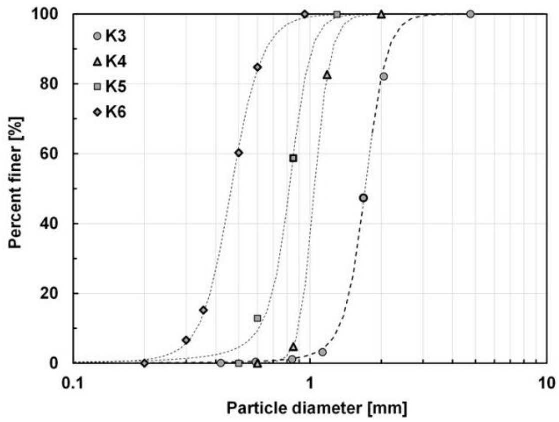

Fig. 1 Particle size distribution curve of tested sands. Data are fitted by Fredlund *et al.* (2000)

Table 2 Index Properties of tested sands

Type	G_s	D_{50} (mm)	D_{10} (mm)	C_u	e_{max}	e_{min}	S_a (cm^2/g)
K3	2.65	1.65	1.30	1.13	1.08	0.72	13.99
K4	2.65	1.01	0.87	1.19	1.08	0.71	23.02
K5	2.65	0.80	0.54	1.47	1.07	0.69	30.05
K6	2.65	0.47	0.33	1.52	1.03	0.66	51.46

Note: G_s = specific gravity; D_{50} = median particle size; D_{10} = effective particle size; C_u = uniformity coefficient; e_{max} = maximum void ratio; e_{min} = minimum void ratio; and S_a = specific surface

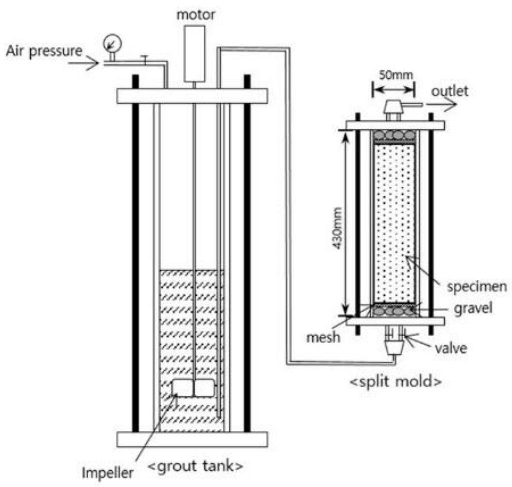

Fig. 2 Schematic drawing of the sample preparation equipment

this study, including the transparent split mold, grouting tank, and air compressor, which is similar to the experimental setup of Dano *et al.* (2004) and Avci and Mollamahmutoğlu (2016). The dimensions of the split mold are 50 mm in inner diameter and 450 mm in height. To reduce bleeding, a 3% and 5% bentonite (Duksan, South Korea) of dry cement mass was added in the preparation of cement suspension, and all cement suspensions (i.e., pure grout) were prepared with the following processes: the predetermined amount of the bentonite was mechanically mixed with deionized water corresponding to 30% of the weight of a target W/C for 5 minutes (Azadi *et al.* 2017); the remaining amount of water and predetermined amount of the microfine cement (or OPC) were poured into the bentonite slurry, and the mixture was mixed for another 5 minutes with a mechanical stirrer. Then, the suspension was transferred into the grout tank and mixed with a speed of 600 rpm to prevent segregation.

To prepare a homogeneous sand specimen, a water pluviation method was used in this study (Chaney and Mulilis 1978). Coarse gravel of 10 mm in thickness and wire mesh were placed at the top and bottom of the mold to avoid segregation and to inject the grout suspension uniformly. A rubber hammer was used to tap the specimens, targeting three different relative densities (i.e., *Dr* = 30, 50, and 70%) of tested sand. After the sand column in the mold was completely built, the grout was injected into the bottom of the sand column. When the volume of injected suspension reached two times void volume of the sand in the column, the injection was finished (Avci and Mollamahmutoğlu 2016). The maximum injection pressure was less than 700 kPa in this study, preventing fracturing or particle movement during injection (Mahabadi and Jang 2017). After injection, the specimens were kept in the mold for 3 days. After 3 days, grouted specimen was detached from the mold and cut to a height of 110 mm. Note that a lubricant lightly covered the inside of the mold for easy detachment of specimens from the mold. Then each specimen was stored and cured under a submerged condition with 23℃ (±0.5℃) for 7, 14, and 28 days in a sealed container.

3.3 Testing methods

Three different W/C ratios of 1.0, 1.5, and 2.0 were selected for all experiments in this study, including the bleeding test, viscosity measurement, and unconfined compression test.

For the bleeding test (ASTM-C940-98a 2003), the cement suspension was poured into a 1000 mL graduated cylinder until the volume of the suspension reached 800±10 mL. The bleeding was measured at 15 minutes intervals for the first 60 minutes, and then bleeding values were read every 1 hour until the suspension was stable.

A rheometer (Merlin Co.) equipped with a four-bladed vane was used to measure the viscosity of the suspensions. The dimensions of the vane were 14 mm in length, 1 mm in thickness, and 30 mm in height. The stress ramp technique was used to evaluate an apparent viscosity of the suspension in this study (Yoon and El Mohtar 2014). At each step, a constant stress level was maintained for 20 seconds and the apparent viscosity was calculated based on the shear rate. The viscosity reaches an equilibrium state (steady state) at a high shear rate and presents a constant apparent viscosity. Because both the bleeding and viscosity of the suspension are sensitive to temperature, all tests were performed at a temperature 23 ℃ (± 0.5 ℃).

An unconfined compression test was performed using a Universal Testing Machine with a capacity of 20 kN at a loading rate of 1 mm/min for cured pure grouts and grouted sands at the end of each curing period (i.e., 3, 7, 14, and 28 days). The top and bottom of the testing specimens were

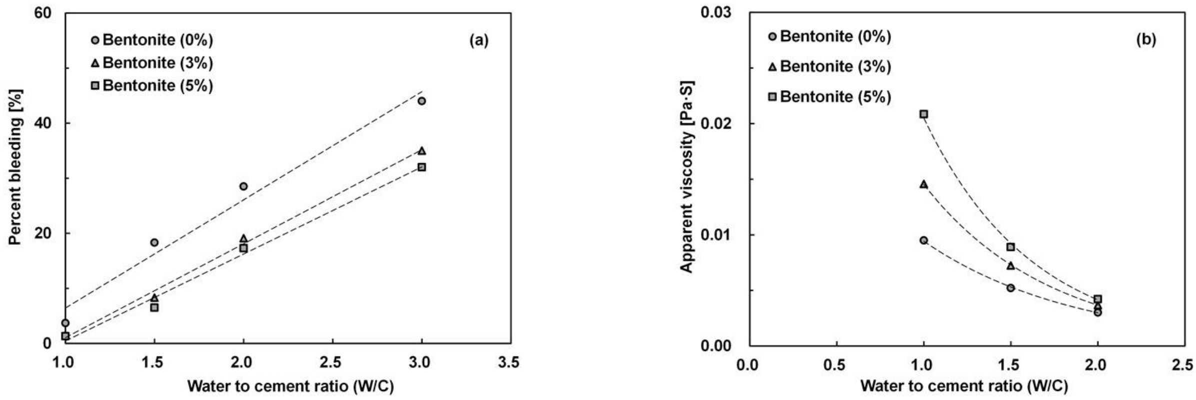

(a) (b)

Fig. 3 (a) Bleeding and (b) apparent viscosity of the microfine cement suspensions with various W/C and bentonite contents

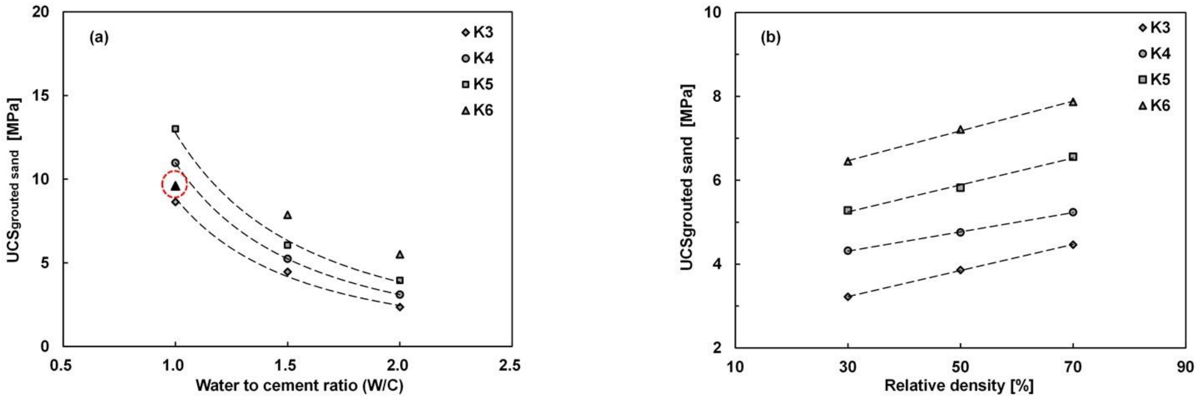

(a) (b)

Fig. 4 Evolution of UCS of sands with four different median particle sizes grouted with microfine cement: (a) effect of W/C for *Dr* = 70% and (b) effect of relative density for W/C=1.5

covered with an unbonded cap to apply uniform stress. Unconfined compression tests at a given testing condition were conducted more than three times, and the average value is reported in this study.

4. Results and analysis

4.1 Bleeding and viscosity of the suspension

The bleeding values of cement suspension generally increases with an increase in W/C (Mirza *et al.* 2013), and the results of this study in Fig. 3(a) also indicate an almost linear increase in bleeding with an increase in W/C. Because the measured bleeding values of tested microfine cement are greater than 18% when the W/C is greater than 1.5, the bentonite was added in the preparation of cement suspension in this study. Thus, the bleeding and apparent viscosity of the microfine cement suspensions were measured as the function of both W/C and bentonite content in Fig. 3. It can be observed in Fig. 3(a) that the bleeding of the grout containing 3% and 5% bentonite based on the dry mass of microfine cement decreases approximately 15% and 20%, respectively, in comparison to the bleeding of the microfine cement without bentonite. This decrease in bleeding with an inclusion of bentonite can be attributed to the fact that the bentonite can absorb free water. In addition, due to the electrochemical reaction between cement particles and bentonite, the bleeding effect can be reduced by adding bentonite in the cement suspension (De Paoli *et al.* 1992).

The viscosity of microfine cement suspension increases exponentially as W/C decreases (Fig. 3(b)). The suspensions containing 3% and 5% bentonite at W/C = 1 are approximately 1.3 and 2.1 times greater than the viscosity of the suspension without bentonite, respectively. It is presumed that the state of dispersion between cement particles and bentonite is improved due to electrochemical reaction with increasing bentonite content (De Paoli *et al.* 1992). Although the bleeding can be reduced by increasing the amount of bentonite contents, high bentonite content causes high apparent viscosity that leads to filtration and uplift of the specimen surface due to high injection pressure (Bruce 1997; Markou and Droudakis 2013). Therefore, 3% of bentonite was added into the cement suspension in this study based on the consideration of both reducing bleeding and the minor increase in viscosity. Consequently, all the reported UCS values in this study are based on the cement suspension containing 3% bentonite.

4.2 Unconfined compressive strength

As mentioned earlier, one of the main variables determining the UCS of grouted sand ($UCS_{grouted\ sand}$) is

UCS of cured pure grout (UCS_{pure}) or W/C of the grout (Dano *et al.* 2004, Schwarz and Chirumalla 2007, Schwarz and Krizek 1994, Zebovitz *et al.* 1989). Fig. 4(a) presents the evolution of UCS as a function of W/C for all tested specimens ($Dr \approx 70\%$) grouted with the microfine cement at 28 days of curing. The UCS of the specimen increases exponentially with a decrease in W/C, which is similar to previous studies (Dano *et al.* 2004, Mollamahmutoglu and Avci 2015, Schwarz and Krizek 1994, Zebovitz *et al.* 1989) because the strength of the cementation contact bonds between sand particles can be increased with decreasing W/C (Choo *et al.* 2018, Choo *et al.* 2017, Markou and Droudakis 2013).

Additionally, it can be observed in Fig. 4(a) that UCS of tested materials generally increases with decreasing median particle size (D_{50}) of the sand because of an increase in specific surface with a decrease in particle size. In other words, sand particles with larger specific surface can effectively adsorb the cement particles, thus a strong cementation bond can be developed with an increase in specific surface (or with a decrease in particle size) (Choo *et al.* 2017, Ismail *et al.* 2002, Yang and Salvati 2010). However, the UCS values of K6 sand (D_{50} = 0.47 mm) are lower than those of K4 sand (D_{50} = 1.01 mm) and K5 sand (D_{50} = 0.80 mm) in the case of W/C = 1 (Fig. 4(a)). This unexpected observation can be explained by the filtration phenomenon: due to the small pore size (or small particle size) and high viscosity of cement grout, the cement particles cannot be efficiently injected into the column of K-6 sand, leading to weak bonds between sand particles (Akbulut and Saglamer 2002, Eklund and Stille 2008, Markou and Droudakis 2013, Mollamahmutoglu and Avci 2015). Therefore, experimental results for K6 sand with W/C=1 are excluded in the estimation of the UCS of microfine cement grouted sand.

Fig. 4(b) shows the effect of relative density (Dr) or porosity (n) on the evolution of the UCS of specimens grouted with microfine cement at W/C = 1.5. UCS tends to increase with increasing Dr (or with decreasing n) (Avci and Mollamahmutoğlu 2016, Clough *et al.* 1981, Huang and Airey 1998) because the number of sand particle contacts within a certain volume increases with increasing Dr or with decreasing n, resulting in an increased number of cementation contact bonds between sand particles. Similar tendencies were observed for other W/C ratios.

5. Discussions

5.1 Estimating UCS of microfine cement grouted sand

Because UCS of ungrouted pure sand with negligible cohesion can be assumed to be zero (Dano *et al.* 2004), Case 1 in Table 1can be rewritten as

$$\frac{UCS_{grouted\ sand}}{1\ MPa} = A_{soil}\left(\frac{UCS\ _{pure}}{1\ MPa}\right)^{N} \tag{2}$$

where A_{soil} = UCS of grouted sand ($UCS_{grouted\ sand}$) when the UCS of cured pure grout (UCS_{pure}) = 1 MPa; and N = exponent capturing the dependency of the $UCS_{grouted\ sand}$ on UCS_{pure}. It is assumed in Eqs. (2) that $UCS_{grouted\ sand}$ can be estimated with two fitting parameters (A_{soil} and N), which are related to the properties of soils and UCS_{pure}. Therefore, the following part focuses on the estimation of UCS_{pure} and on the developments of relationships between the properties of sands and two fitting parameters.

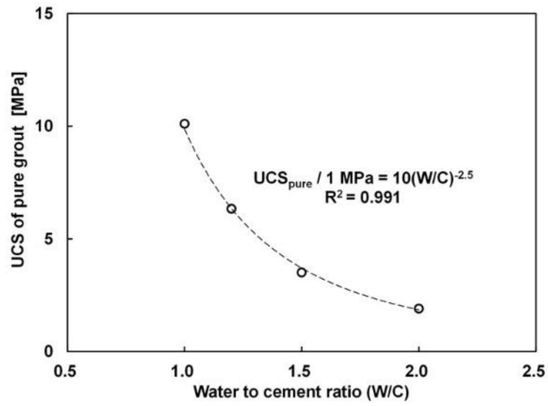

Fig. 5 Relationship between UCS of cured pure grout (microfine cement) at 28 days of curing time and W/C

Fig. 5 shows the variation of UCS_{pure} (UCS of pure microfine cement suspension) cured for 28 days according to W/C. It can be observed in Fig. 5 that UCS values increase significantly with decreasing W/C of the suspensions in agreement with the results of previous studies (Avci and Mollamahmutoğlu 2016, Dano *et al.* 2004, Kaga and Yonekura 1991, Pantazopoulos and Atmatzidis 2012). Note that Fig. 5 demonstrates that UCS_{pure} is directly determined by W/C; thus, UCS_{pure} in Eqs. (2) can be expressed as

$$\frac{UCS_{pure}}{1\ MPa} = A'\left(\frac{W}{C}\right)^{N'} = 10\left(\frac{W}{C}\right)^{-2.5} \tag{3}$$

where A' and N' = fitting parameters. The determined values of A' and N' of tested microfine cement are 10 and -2.5, respectively. However, A' and N' vary with the cement type, manufacture, chemical composition, specific surface, and others. Therefore, to estimate the UCS_{pure} using Eqs. (3), the determination of A' and N' is a prerequisite.

5.2 Investigating A_{soil} and N for estimating UCS of grouted sand

To figure out A_{soil} and N values in Eqs. (2) of tested sands, the relationship between $UCS_{grouted\ sand}$ and UCS_{pure} is investigated in Fig. 6. The comparison of four sands with varying D_{50} at three different relative densities demonstrates that both A_{soil} and N are affected by sand type (i.e., particle size, particle gradation, specific surface, and others) and relative density (or porosity). Most notably, Fig. 6 demonstrates that, with a decrease in particle size (or increase in specific surface) and with an increase in relative density (or decrease in porosity), the A_{soil} increases, but N decreases.

As mentioned previously, the exponent N in Eqs. (2) implies a sensitivity of $UCS_{grouted\ sand}$ to the changes of UCS_{pure}. To estimate N in Eqs. (2), Kaga and Yonekura

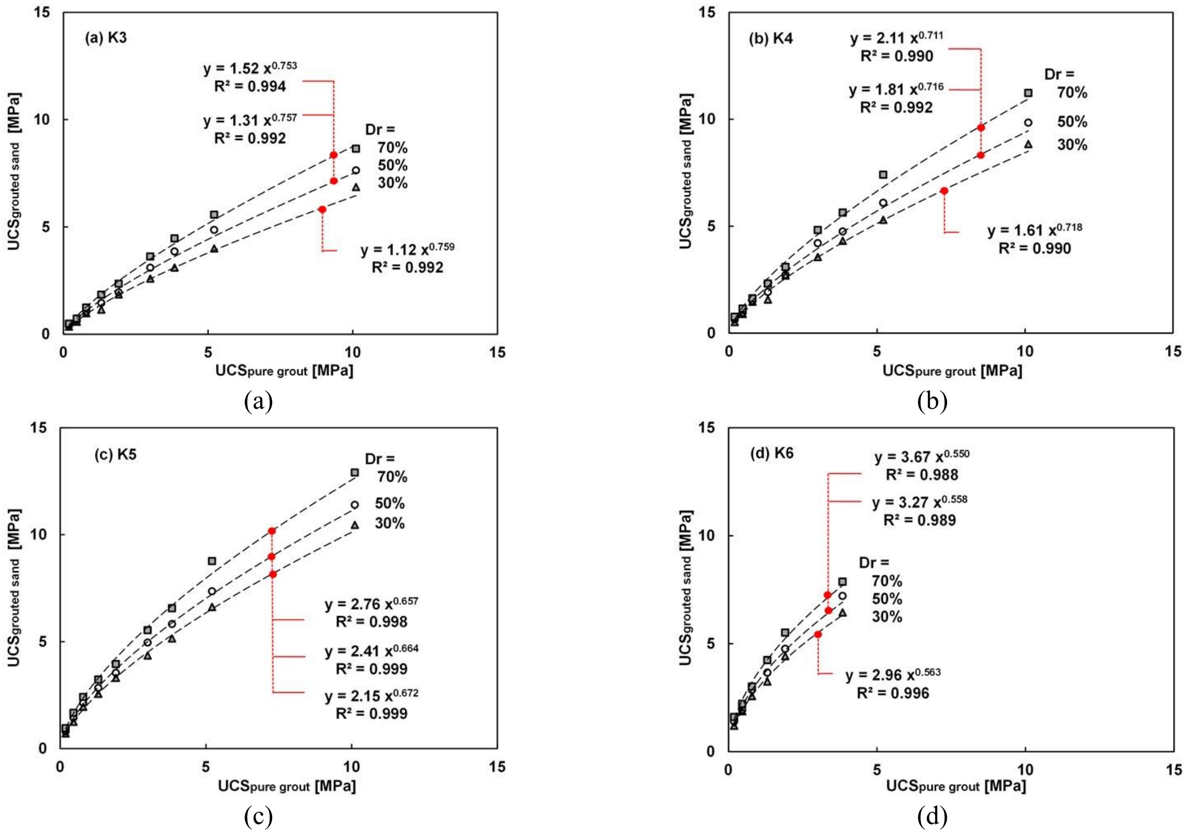

Fig. 6 Relationship between UCS of grouted sand and UCS of pure grout for tested four sands: (a) K3 sand (D_{50} = 1.65 mm), (b) K4 sand (D_{50} = 1.01 mm), (c) K5 sand (D_{50} = 0.80 mm) and (d) K6 sand (D_{50} = 0.47 mm). A_{soil} and N values in Eqs. (2) are included in the figure.

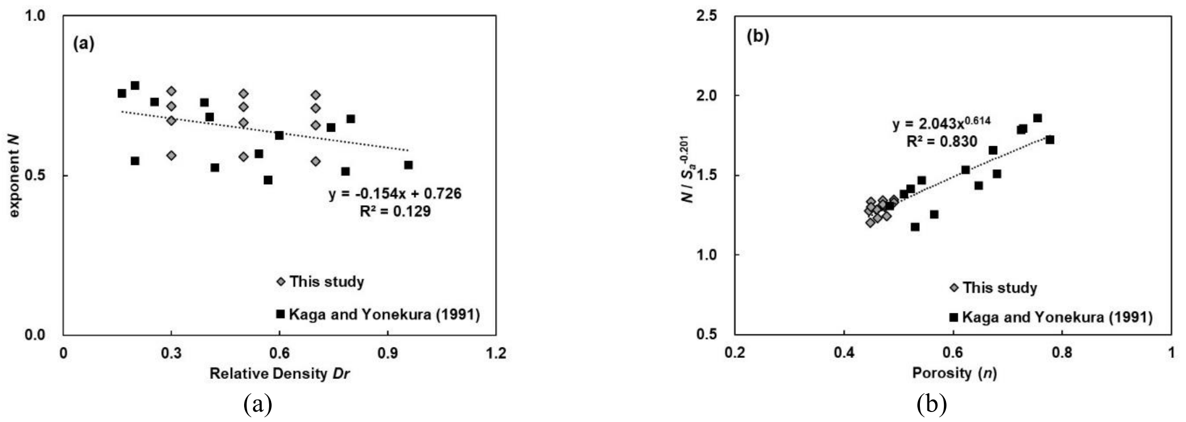

Fig. 7 Estimating exponent N using soil properties (a) effect of relative density and (b) effects of porosity and specific surface

(1991) suggested a linear relationship between relative density (Dr) and N, which is $N = 0.727 - 0.2 \cdot Dr$. Therefore, the N values of this study (i.e., the measured N) and those of Kaga and Yonekura (1991) were plotted as a function of Dr in Figure 7(a). The relationship between N and Dr using data of this study and that of Kaga and Yonekura (1991), which is $N = 0.726 - 0.154 \cdot Dr$, is comparable with the existing formula of Kaga and Yonekura (1991). However, as reflected in very low R^2 value in Fig. 7(a), N-Dr relationship is very weak because the results of this study demonstrate that the exponent N is dependent not only on packing condition, but also on specific surface (or particle size) (Fig. 6). Note that the strength gain due to the grouting originates from the cementation bonding between sand particles. In the case of sands with large pore size and large pore area, the strength gain due to grouting will be very small when W/C is high (or when UCS of pure grout is small) because the large part of grout suspension just fills the pore space between sand particles. However, with an increase in cement content (or decrease in W/C), the grout suspension can significantly contribute to the strength gain of sand through the formation of cementation bonding between sand particles.

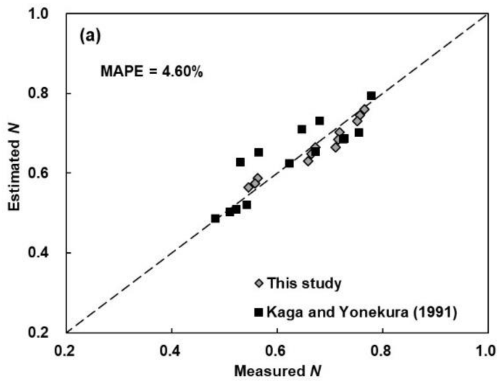

(a)

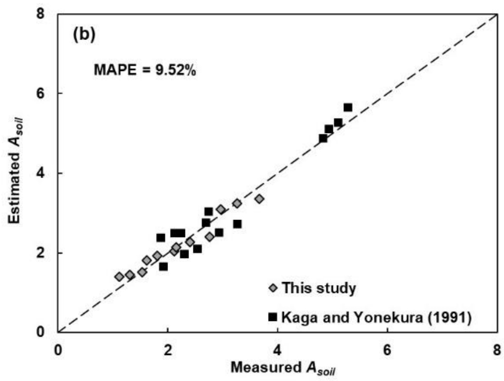

(b)

Fig. 8 Comparison between the measured and estimated fitting parameters in Eqs. (2): (a) comparison of N values and (b) comparison of A_{soil} values

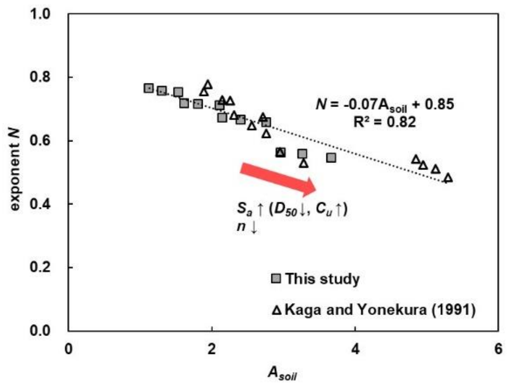

Fig. 9 Relationship between A_{soil} and N based on the results of this study and Kaga and Yonekura (1991)

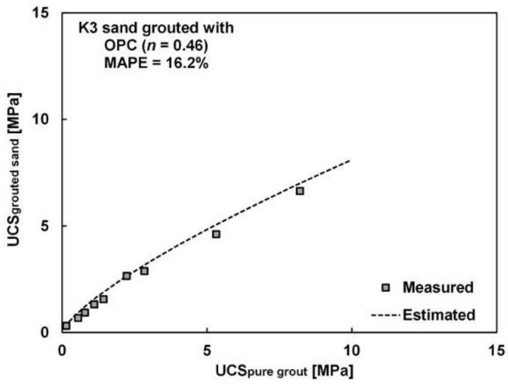

Fig. 10 Comparison between the measured and estimated UCS of K3 with Dr = 50% grouted by OPC

Therefore, sands with large pore size and large pore area can show great dependency on the change in UCS_{pure} reflecting large N values for these sands. In contrast, in the case of sands with small pore size and small pore area, the cementation contact bond can be formed at relatively high W/C; therefore, these sands show relatively small N values, resulting from the relatively small change in $UCS_{grouted\ sand}$ according to the change in UCS_{pure}.

The above explanation demonstrates the strong dependency of N on pore area and pore size. The area of pore space can be captured by the porosity (or relative density), and the size of pore space can be captured by a specific surface (or particle diameter). Therefore, both porosity (n) and the specific surface (S_a) can affect the value of N. Consequently, using the data in Fig. 6 and data in Kaga and Yonekura (1991), multiple regression analysis was performed to investigate the effect of S_a and n on N, and the following relationship was obtained (Fig. 7(b))

$$N = 2.043 \times \left(\frac{S_a}{1\ cm^2/g}\right)^{-0.201} \times n^{0.614} \quad (R^2 = 0.830) \qquad (4)$$

Note that N estimating formulas using D_{10} or D_{50} instead of S_a, and using Dr instead of n can also be developed; however, an N estimating formula based on S_a and n shows the highest R^2 value, reflecting the importance of S_a and n to the proper estimation of N value. Consistent with the explanation shown above, Eqs. (4) and Fig. 7(b) demonstrate an increase in N with a decrease in S_a, reflecting an increase in pore size, and with an increase in n, reflecting an increase in pore area. Most notably, compared to Fig. 7(a), a strong N estimating formula can be developed by employing S_a and n, reinforcing the strong dependency of N on both packing condition and specific surface (Fig. 7(b)). The comparison between the measured N and estimated N (Eqs. (4)) using data of this study and data of Kaga and Yonekura (1991) is shown in Fig. 8(a). To quantify the difference between the measured and estimated N values, the mean absolute percentage error (MAPE), from Eqs. (5), is also included in Fig. 8(a).

$$\mathrm{MAPE} = \frac{1}{M}\sum_{i=1}^{M}\left|\frac{measured\ \ value - estimated\ \ value}{measured\ \ value}\right| \qquad (5)$$

where M = number of data. Fig. 8(a) demonstrate that Eqs. (4) yields a good agreement between the measured and estimated N with the MAPE of around 4.6%.

A_{soil} in Eqs. (2) represents the UCS of grouted sand when the UCS of cured pure grout is 1 MPa; therefore, factors affecting the strength of cemented sands (e.g., cementation level, porosity, sand type, particle size, and specific surface) will determine the magnitude of A_{soil}. Note that the UCS estimating formulas in Table 1 demonstrate that specific surface (or particle size), porosity, and UCS of pure grout determine the UCS of grouted sands. Therefore, using the data in Fig. 6 and data in Kaga and Yonekura

(1991), multiple regression analysis was performed to investigate the effect of specific surface (S_a) and porosity (n) on A_{soil}, and the following relationship was obtained

$$A_{soil} = 0.10 \times \left(\frac{S_a}{1\ cm^2/g}\right)^{0.62} \times n^{-1.30} \quad (R^2 = 0.912) \quad (6)$$

Similar to the analysis for estimating N value, A_{soil} estimating formulas using D_{10} or D_{50} instead of S_a and using Dr instead of n can also be developed; however, an A_{soil} estimating formula based on S_a and n shows the highest R^2 value; therefore, A_{soil} estimating formula based on S_a and n is only reported in this study. This strong dependency of A_{soil} on S_a and n can be attributed to the following facts. First, S_a determines the area of the sand particle that the cement particles can adsorb; thus, the strength of cementation bonding increases with an increase in S_a. Second, n reflects the coordination number that determines the number of cementation bondings between sand particles. Thus, with a decrease in n, the number of cementation bonding increases. Consequently, with an increase in S_a and a decrease in n, the A_{soil} value increases (Eqs. (6)). Note that Kaga and Yonekura (1991) experimentally expressed A_{soil} as the function of the specific surface per unit volume of sand; however, the estimations of A_{soil} using the formula of Kaga and Yonekura (1991) are not matched with the measured A_{soil} values in this study. Thus, the A_{soil} estimating formula of Kaga and Yonekura (1991) is not further discussed in this study. Fig. 8(b) shows the comparison between the measured A_{soil} and estimated A_{soil} (Eqs. (6)) using the data of this study and of Kaga and Yonekura (1991). A good agreement between the measured and estimated A_{soil} with a MAPE of around 9.5% can be found in Fig. 8(b).

Because both A_{soil} and N are affected by the same soil properties (Eqs. (4) and (6)), the direct relationship between A_{soil} and N is investigated in Fig. 9. Fig. 9 indicates that sands with high S_a and low n will have greater A_{soil} but smaller N, and the A_{soil} and N are inversely proportional according to the following relationship

$$N = -0.07 \cdot A_{soil} + 0.85 \quad (7)$$

Eq. (7) highlights that in the case of sands with high S_a and low n, the target UCS can be achieved using grout with a relatively high W/C (or grout with relatively low strength). However, in the case of sands with low S_a and high n, relatively low W/C is required to achieve the target UCS.

5.3 Effect of grout type on the suggested equation

It is assumed in this study that both A_{soil} and N in Eqs. (2) are soil-related properties; therefore, A_{soil} and N should not be affected by the characteristics of grout. To figure out the effect of cement type on the validity of the suggested A_{soil} and N estimating formulas (Eqs. (4) and (6)) for the estimation of $UCS_{grouted\ sand}$, K3 sand with Dr = 50% (or n = 0.46) was grouted with Ordinary Portland cement (OPC) at W/C = 1.0, 1.5, and 2.0. Note that the grouting with OPC was conducted only on K3 sand with D_{50} = 1.65 mm to avoid the filtration effect. Because UCS_{pure} can be varied with the grout types, the UCS of pure OPC cured for 28 days was first determined as the function of W/C

$$\frac{UCS_{pure}}{1\ MPa} = A'\left(\frac{W}{C}\right)^{N'} = 8\left(\frac{W}{C}\right)^{-2.5} \quad (8)$$

The determined A' and N' values for the tested OPC are 8 and -2.5, respectively, reflecting that the UCS of OPC is smaller than the UCS of microfine cement at a given W/C (Pantazopoulos *et al.* 2012). By combining Eqs. (2), (4), (6), and (8), the UCS of the grouted sand with OPC are estimated and compared with the measured values in Fig. 10. Fig. 10 shows that the estimated UCS values are reasonably matched with the measured UCS (MAPE = 16.2%), reflecting that 1) the suggested A_{soil} and N estimating formulas can be used for the proper estimation of $UCS_{grouted\ sand}$; and 2) A_{soil} and N in Eqs. (2) are determined by the physical properties of sand, and the effect of grout type on A_{soil} and N is negligible. In this aspect, it is remarkable that Eqs. (4) and (6) are based on the results of both this study, which used microfine cement as the grout, and Kaga and Yonekura (1991), which used a silicate as the grout. Thus, Eqs. (4) and (6) already imply that the suggested A_{soil} and N estimating formulas depend only on the characteristics of sand.

6. Conclusions

For quality control and the economical design of grouted sand, the prior establishment of an empirical unconfined compressive strength (UCS) estimating formula is very important. Therefore, this experimental investigation aims at developing UCS estimating formula for grouted sand ($UCS_{grouted\ sand}$) based on the physical properties of sands and the UCS of cured pure grout (UCS_{pure}). The key findings from this study are summarized:

1) $UCS_{grouted\ sand}$ can be expressed as the power function of UCS_{pure}: $UCS_{grouted\ sand}$ / 1 MPa = $A_{soil} \cdot (UCS_{pure}$ / 1 MPa$)^N$.

2) The exponent N, which indicates the sensitivity of $UCS_{grouted\ sand}$ to the changes of UCS_{pure}, is strongly dependent on the pore size and pore area. Because the area of pore space can be captured by the porosity (n) and the size of pore space can be captured by specific surface (S_a), the exponent N is expressed as the function of n and S_a.

3) S_a determines the area of the sand particle that the cement particles can adsorb, and n reflects the coordination number that determines the number of cementation bonding between sand particles. Therefore, A_{soil}, which represents $UCS_{grouted\ sand}$ when UCS_{pure} =1, is expressed as the function of n and S_a.

4) Sands with high S_a and low n show greater A_{soil} but smaller N, and an inversely proportional relationship has been shown between A_{soil} and N.

5) The suggested A_{soil} and N estimating formulas depend only on the characteristics of sand.

Acknowledgments

This research was supported by the National Research Foundation of Korea (NRF) grant funded by the Korean government (NRF-2017R1C1B2004036).

References

Abramson, L.W., Lee, T.S., Sharma, S. and Boyce, G.M. (2002), *Slope Stability and Stabilization Methods*, John Wiley & Sons., Hoboken, New Jersey, U.S.A.

Akbulut, S. and Saglamer, A. (2002), “Estimating the groutability of granular soils: A new approach”, *Tunn. Undergr. Sp. Technol.*, **17**(4), 371-380. https://doi.org/10.1016/S0886-7798(02)00040-8.

ASTM-C940-98a (2003), “Standard test method for expansion and bleeding of freshly mixed grouts for preplaced-aggregate concrete in the laboratory”, Annual Book of ASTM Standards, ASTM, West Conshohocken, Pennsylvania, U.S.A.

Avci, E. and Mollamahmutoğlu, M. (2016), “UCS roperties of superfine cement–grouted sand”, *J. Mater. Civ. Eng.*, **28**(12), 06016015. https://doi.org/10.1061/(ASCE)MT.1943-5533.0001659.

Azadi, M.R., Taghichian, A. and Taheri, A. (2017), “Optimization of cement-based grouts using chemical additives”, *J. Rock Mech. Geotech. Eng.*, **9**(4), 623-637., https://doi.org/10.1016/j.jrmge.2016.11.013.

Brachman, R.W.I., Martin, C.D. and Gilliss, S.A. (2004), “Grout field trials in outwash sands”, *Can. Geotech. J.*, **41**(1), 1-11. https://doi.org/10.1139/t03-069.

Bruce, D.A., Littlejohn, G.S. and Naudts, A. (1997), “Grouting materials for ground treatment: A practitioner’s guide”, *Proceedings of the Sessions Sponsored by the Grouting Committee of the Geo-Institute of the American Society of Civil Engineers in Conjuction with the Geo-Logan'97 Conference*, Logan, Utah, U.S.A., July.

Celik, F. (2019), “The observation of permeation grouting method as soil improvement technique with different grout flow models”, *Geomech. Eng.*, **17**(4), 367-374. https://doi.org/10.12989/gae.2019.17.4.367.

Chaney, R. and Mulilis, J. (1978), “Suggested method for soil specimen remolding by wet-raining”, *Geotech. Test. J.*, **1**(2), 107-108., https://doi.org/10.1520/GTJ10378J.

Chang, M.H., Mao, T.W. and Huang, R.C. (2016), “A study on the improvements of geotechnical properties of in-situ soils by grouting”, *Geomech. Eng.*, **10**(4), 527-546. http://dx.doi.org/10.12989/gae.2016.10.4.527.

Choo, H., Lee, W. and Lee, C. (2018), “Overconsolidation and Cementation in Sands: Impacts on Geotechnical Properties and Evaluation Using Dilatometer Tests”, *Geotech. Test. J.*, **41**(5), 915-929., https://doi.org/10.1520/GTJ20170368.

Choo, H., Lee, W., Lee, C. and Burns, S.E. (2018), “Estimating porosity and particle size for hydraulic conductivity of binary mixed soils containing two different-sized silica particles”, *J. Geotech. Geoenviron. Eng.*, **144**(1), 04017104. https://doi.org/10.1061/(ASCE)GT.1943-5606.0001802.

Choo, H., Nam, H. and Lee, W. (2017), “A practical method for estimating maximum shear modulus of cemented sands using unconfined compressive strength”, *J. Appl. Geophys.*, **147**, 102-108. https://doi.org/10.1016/j.jappgeo.2017.10.012.

Clough, G.W., Sitar, N., Bachus, R.C. and Rad, N.S. (1981), “Cemented sands under static loading”, *J. Geotech. Eng. Div.*, **107**(6), 799-817.

Consoli, N.C., Foppa, D., Festugato, L. and Heineck, K.S. (2007), “Key parameters for strength control of artificially cemented soils”, *J. Geotech. Geoenviron. Eng.*, **133**(2), 197-205. https://doi.org/10.1061/(ASCE)1090-0241(2007)133:2(197).

Dano, C., Hicher, P.Y. and Tailliez, S. (2004), “Engineering properties of grouted sands”, *J. Geotech. Geoenviron. Eng.*, **130**(3), 328-338. https://doi.org/10.1061/(ASCE)1090-0241(2004)130:3(328).

De Paoli, B., Bosco, B., Granata, R. and Bruce, D. (1992), “Fundamental observations on cement based grouts (1): traditional materials”, *Proceedings of the ASCE Specialty Conference on Grouting, Soil Improvement and Geosynthetics*, New Orleans, Louisiana, U.S.A., February.

Eklund, D. and Stille, H. (2008), “Penetrability due to filtration tendency of cement-based grouts”, *Tunn. Undergr. Sp. Technol.*, **23**(4), 389-398. https://doi.org/10.1016/j.tust.2007.06.011.

Fredlund, M.D., Fredlund, D. and Wilson, G.W. (2000), “An equation to represent grain-size distribution”, *Can. Geotech. J.*, **37**(4), 817-827. https://doi.org/10.1139/t00-015.

Gallagher, P.M. and Mitchell, J.K. (2002), “Influence of colloidal silica grout on liquefaction potential and cyclic undrained behavior of loose sand”, *Soil Dyn. Earthq. Eng.*, **22**(9-12), 1017-1026. https://doi.org/10.1016/S0267-7261(02)00126-4

Gallagher, P.M., Pamuk, A. and Abdoun, T. (2007), “Stabilization of liquefiable soils using colloidal silica grout”, *J. Mater. Civ. Eng.*, **19**(1), 33-40. https://doi.org/10.1061/(ASCE)0899-1561(2007)19:1(33).

Gopinathan, S. and Anand, K.B. (2018), “Properties of cement grout modified with ultra-fine slag”, *Front. Struct. Civ. Eng.*, **12**(1), 58-66., https://doi.org/10.1007/s11709-017-0383-0.

Hoek, E. (2001), “Big tunnels in bad rock”, *J. Geotech. Geoenviron. Eng.*, **127**(9), 726-740. https://doi.org/10.1061/(ASCE)1090-0241(2001)127:9(726).

Hsiao, D.H., Phan, V.T.A. and Huang, C.C. (2016), “An experimental investigation on dynamic properties of various grouted sands”, *Geomech. Eng.*, **10**(1), 77-94., http://dx.doi.org/10.12989/gae.2016.10.1.077.

Huang, J. and Airey, D. (1998), “Properties of artificially cemented carbonate sand”, *J. Geotech. Geoenviron. Eng.*, **124**(6), 492-499. https://doi.org/10.1061/(ASCE)1090-0241(1998)124:6(492).

Ismail, M.A., Joer, H.A., Randolph, M.F. and Meritt, A. (2002), “Cementation of porous materials using calcite”, *Geotechnique*, **52**(5), 313-324. https://doi.org/10.1680/geot.2002.52.5.313.

Kaga, M. and Yonekura, R. (1991), “Estimation of strength of silicategrouted sand”, *Soils Found.*, **31**(3), 43-59. https://doi.org/10.3208/sandf1972.31.3_43.

Li, S.C., Sha, F., Liu, R.T., Zhang, Q.S. and Li, Z.F. (2017), “Investigation on fundamental properties of microfine cement and cement-slag grouts”, *Construct. Build. Mater.*, **153**, 965-974. https://doi.org/10.1016/j.conbuildmat.2017.05.188.

Mahabadi, N. and Jang, J. (2017), “The impact of fluid flow on force chains in granular medium”, *Appl. Phys. Lett.*, **110**(4), 041907. https://doi.org/10.1063/1.4975065.

Markou, I. and Droudakis, A. (2013), “Factors affecting engineering properties of microfine cement grouted sands”, *Geotech. Geol. Eng.*, **31**(4), 1041-1058. https://doi.org/10.1007/s10706-013-9631-9.

Mirza, J., Saleh, K., Langevin, M.A., Mirza, S., Bhutta, M.A.R. and Tahir, M.M. (2013), “Properties of microfine cement grouts at 4 degrees C, 10 degrees C and 20 degrees C”, *Construct. Build. Mater.*, **47**, 1145-1153. https://doi.org/10.1016/j.conbuildmat.2013.05.026.

Mollamahmutoglu, M. and Avci, E. (2015), “Effectiveness of microfine portland cement grouting on the strength and permeability of medium to fine sands”, *Periodica Polytechnica Civ. Eng.*, **59**(3), 319-326., https://doi.org/10.3311/PPci.7674.

Nonveiller, E. (2013), *Grouting Theory and Practice*, Elsevier, Amsterdam, The Netherlands

Ozgurel, H.G. and Vipulanandan, C. (2005), “Effect of grain size and distribution on permeability and mechanical behavior of acrylamide grouted sand”, *J. Geotech. Geoenviron. Eng.*, **131**(12), 1457-1465. https://doi.org/10.1061/(ASCE)1090-0241(2005)131:12(1457).

Pantazopoulos, I. and Atmatzidis, D. (2012), “Dynamic properties of microfine cement grouted sands”, *Soil Dyn. Earthq. Eng.*, **42**, 17-31. https://doi.org/10.1016/j.soildyn.2012.05.017.

Pantazopoulos, I., Markou, I., Christodoulou, D., Droudakis, A., Atmatzidis, D., Antiohos, S. and Chaniotakis, E. (2012), "Development of microfine cement grouts by pulverizing ordinary cements", *Cement Concrete Compos*., **34**(5), 593-603. https://doi.org/10.1016/j.cemconcomp.2012.01.009.

Pantazopoulos, I.A. and Atmatzidis, D.K. (2012), "Dynamic properties of microfine cement grouted sands", *Soil Dyn. Earthq. Eng*., **42**, 17-31. https://doi.org/10.1016/j.soildyn.2012.05.017.

Santamarina, J.C., Klein, K.A. and Fam, M.A. (2001), *Soils and Waves: Particulate Materials Behavior, Characterization and Process Monitoring*, J. Wiley & Sons, Chichester, England, U.K.

Schwarz, L.G. and Chirumalla, M. (2007), "Effect of injection pressure on permeability and strength of microfine cement grouted sand", *Proceedings of the GeoDenver 2007*, *New Peaks in Geotechnics*, Denver, Colorado, U.S.A., February.

Schwarz, L.G. and Krizek, R.J. (1994), "Effect of preparation technique on permeability and strength of cement-grouted sand", *Geotech. Test. J*., **17**(4), 434-443. https://doi.org/10.1520/GTJ10304J.

Sunitsakul, J., Sawatparnich, A. and Sawangsuriya, A. (2012), "Prediction of unconfined compressive strength of soil–cement at 7 days", *Geotech. Geol. Eng*., **30**(1), 263-268. https://doi.org/10.1007/s10706-011-9460-7.

Tinoco, J., Correia, A.G. and Cortez, P. (2011), "Application of data mining techniques in the estimation of the uniaxial compressive strength of jet grouting columns over time", *Construct. Build. Mater*., **25**(3), 1257-1262., https://doi.org/10.1016/j.conbuildmat.2010.09.027.

Van der Stoel, A.E.C. (2001), "Grouting for pile foundation improvement", Ph.D. Thesis, TU Delft, Delft University of Technology., Delft, The Netherlands

Yang, L. and Salvati, L. (2010), "Small strain properties of sands with different cement types", *Proceedings of the 5th International Conference on Recent Advances in Geotechnical Earthquake Engineering and Soil Dynamics and Symposium in Honor of Professor I.M. Idriss*, San Diego, California, U.S.A., May.

Yoon, J. and El Mohtar, C.S. (2014), "Groutability of granular soils using bentonite grout based on filtration model", *Transport Porous Media*, **102**(3), 365-385. https://doi.org/10.1007/s11242-014-0279-6.

Zebovitz, S., Krizek, R. and Atmatzidis, D. (1989), "Injection of fine sands with very fine cement grout", *J. Geotech. Eng*., **115**(12), 1717-1733. https://doi.org/10.1061/(ASCE)0733- 9410(1989)115:12(1717).

Zheng, X., Perreault, F. and Jang, J. (2018), "Fines adsorption on nanoparticle-coated surface", *Acta Geotechnica*, **13**(1), 219-226. https://doi.org/10.1007/s11440-017-0528-2.

GC